

Dynamics of an underdamped Josephson-junction ladder

Seungoh Ryu, Wenbin Yu, and D. Stroud

Department of Physics, Ohio State University, Columbus, Ohio 43210

(Received 21 September 1995)

We show analytically that the dynamical equations for an underdamped ladder of coupled small Josephson junctions can be approximately reduced to the discrete sine-Gordon equation. As numerical confirmation, we solve the coupled Josephson equations for such a ladder in a magnetic field. We obtain discrete-sine-Gordon-like IV characteristics, including a flux flow and a “whirling” regime at low and high currents, and voltage steps that represent a lock-in between the vortex motion and linear “phasons,” and which are quantitatively predicted by a simple formula. At sufficiently high anisotropy, the fluxons on the steps propagate ballistically.

PACS number(s): 05.45.+b, 74.40.+k, 03.20.+i, 74.50.+r

I. INTRODUCTION

The discrete sine-Gordon equation has been used by several groups to model so-called hybrid Josephson ladder arrays [1–3]. Such an array consists of a ladder of parallel Josephson junctions that are inductively coupled together, e.g., by superconducting wires [4]. The sine-Gordon equation then describes the phase differences across the junctions. In an applied magnetic field, this equation predicts remarkably complex behavior, including flux-flow resistance below a certain critical current, and a field-independent resistance above that current arising from so-called “whirling” modes [2]. In the flux-flow regime, the fluxons in this ladder propagate as localized solitons, and the numerically determined IV characteristics exhibit voltage plateaus arising from the locking of solitons to linear “spin wave” modes.

In this paper, we show numerically that most of this behavior is to be found in a model in which the ladder is treated as a network of coupled small junctions arranged along both the edges and the rungs of the ladder. To confirm our numerical results, we derive, within certain approximations, a discrete sine-Gordon equation from our coupled-network model. Kardar [5] has previously carried out such a derivation in the limit of no applied current, but the present work appears to be the first to extend this derivation to the dynamical properties, and to confirm it numerically.

The remainder of this paper is organized as follows. Section II describes the model used, which is followed by our numerical results presented in Sec. III. A brief discussion of the results follows in Sec. IV.

II. MODEL

The ladder consists of coupled superconducting grains, the i th of which has order parameter $\Phi_i = \Phi_0 e^{i\theta_i}$. Grains i and j are coupled by resistively shunted Josephson junctions (RSJ's) with current I_{ij} , shunt resistance R_{ij} , and shunt capacitance C_{ij} , with periodic boundary conditions (see Fig. 1).

The phases θ_i are assumed to evolve according to the

coupled RSJ equations [6] $\hbar\dot{\theta}_i/(2e) = V_i$, $\sum_j M_{ij}\dot{V}_j = I_i^{\text{ext}}/I_c - \sum_j (R/R_{ij})(V_i - V_j) - \sum_j (I_{ij}/I_c) \sin(\theta_{ij} - A_{ij})$. Here the time unit is $t_0 = \hbar/(2eRI_c)$, where R and I_c are the shunt resistance and critical current across a junction in the x direction (see Fig. 1); I_i^{ext} is the external current fed into the i th node; the spatial distances are given in units of the lattice spacing a , and the voltage V_i in units of $I_c R$. $M_{ij} = -4\pi e C I_c R^2 / h$ for $i \neq j$, and $M_{ii} = -\sum_{j \neq i} M_{ij}$, where C is the intergrain capacitance. Finally, $A_{ij} = (2\pi/\Phi_0) \int_i^j \mathbf{A} \cdot d\mathbf{l}$, where \mathbf{A} is the vector potential. We assume N plaquettes in the array, and postulate a current I uniformly injected into each node on the outer edge and extracted from each node on the inner edge of the ring. We also assume a uniform transverse magnetic field $B \equiv f\phi_0/a^2$, and use the Landau gauge $\mathbf{A} = -Bx\hat{y}$.

We now show that, within certain approximations, this model can be reduced to a discrete sine-Gordon equation

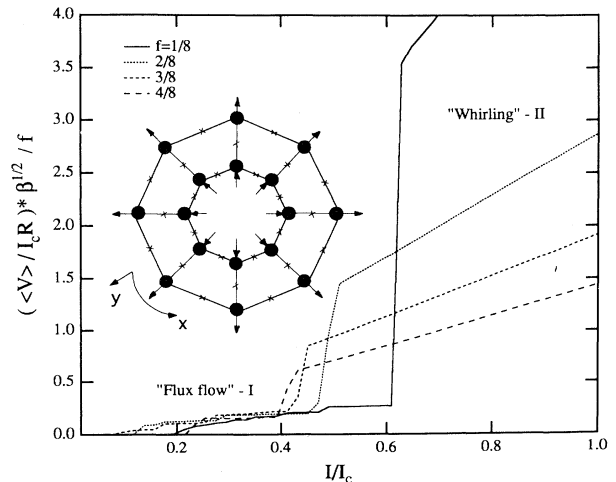


FIG. 1. Calculated IV curves for various values of f in an 8×1 ladder ring. $f \equiv Ba^2/\phi_0 = 1/8$ is the number of flux quanta per plaquette. We use $\beta = 33$ and $\eta_J = 0.71$. Plotted voltages are divided by f . Inset: schematic of ring topology used in simulation. A uniform current is injected into the inner grains and drawn out from the outer grains.

for the *phase differences*. A similar derivation has been given by Kardar [5] in the static case (no applied current). Label each grain by (x, y) where $x/a = 0, \dots, N-1$ and $y/a = 0, 1$. Subtracting the equation of motion for $\theta(x, 1)$ from that for $\theta(x, 2)$, and defining $\Psi(x) = \frac{1}{2}[\theta(x, 1) + \theta(x, 2)]$, $\chi(x) = [\theta(x, 2) - \theta(x, 1)]$, we obtain a differential equation for $\chi(x)$ that is second order in time. This equation may be further simplified using the facts that $A_{x,y;x\pm 1,y} = 0$ in the Landau gauge, and that $A_{x,1;x,2} = -A_{x,2;x,1}$, and by defining the discrete Laplacian $\chi(x+1) - 2\chi(x) + \chi(x-1) = \nabla^2\chi(x)$. Finally, using the boundary conditions, $I^{\text{ext}}(x, 2) = -I^{\text{ext}}(x, 1) \equiv I$, and introducing $\varphi(x) = \chi(x) - A_{x,2;x,1}$, we obtain

$$\begin{aligned} [1 - \eta_c^2 \nabla^2] \beta \ddot{\varphi} &= i - [1 - \eta_r^2 \nabla^2] \dot{\varphi} - \sin(\varphi) + 2\eta_J^2 \\ &\times \sum_{n=\pm 1} \cos\{\Psi(x) - \Psi(x+n)\} \\ &\times \sin\{[\varphi(x) - \varphi(x+n)]/2\}. \end{aligned} \quad (1)$$

Here we have defined a dimensionless current $i = I/I_{cy}$, and anisotropy factors $2\eta_r^2 = R_y/R_x$, $2\eta_c^2 = C_x/C_y$, and $2\eta_J^2 = I_{cx}/I_{cy}$.

We now neglect all combined space and time derivatives of order three or higher. Similarly, we set the cosine factor equal to unity (we have checked numerically that this approximation is valid *a posteriori* in several cases). Finally, we linearize the sine factor in the last term, so that the last summation can be expressed simply as $\nabla^2\varphi$. If these approximations are valid, Eq. (1) reduces to the *discrete driven sine-Gordon equation with dissipation*:

$$\beta \ddot{\varphi} + \dot{\varphi} + \sin(\varphi) - \eta_J^2 \nabla^2 \varphi = i, \quad (2)$$

where $\beta = 4\pi e I_{cy} R_y^2 C_y / h$.

Mathematically, the reduction that leads to Eq. (2) should be accurate so long as the following inequalities hold true:

$$|\nabla^2 \dot{\varphi}| \ll |\dot{\varphi}|, \quad (3)$$

$$|\nabla^2 \ddot{\varphi}| \ll |\ddot{\varphi}|, \quad (4)$$

$$|\Psi(x) - \Psi(x+n)| \ll 1, \quad (5)$$

$$|\varphi(x) - \varphi(x+n)| \ll 1. \quad (6)$$

In general, these equalities should be valid whenever both φ and ψ are slowly varying along the ladder, i.e., in the x direction. In practice, it is difficult to confirm analytically that these conditions will be satisfied, without actually carrying out the numerical calculations. The numerical results, however, suggest that this reduction is quite accurate over most of the parameter range we have investigated. Also, note that even though we are assuming that φ and Ψ are slowly varying, we still retain many effects arising from lattice discreteness, as discussed further below.

III. NUMERICAL RESULTS

To confirm the accuracy of this reduction, we have numerically solved the coupled Josephson equations on an 8×1 ($N = 8$) ring, using a fourth-order Runge-Kutta

algorithm. In general, we find numerically that the phenomena seen in our solutions of the Josephson ladder equations closely resemble previous simulations of the discrete sine-Gordon equation for comparable parameters [1–3].

A. Overview: Flux-flow and whirling regime

Before presenting the numerical solutions, we give a brief overview of what will be displayed. In all cases, we find two distinct voltage regimes: a “flux-flow” regime, characterized by the motion of one or more solitonlike solutions, and a “whirling” regime, dominated by single-junction behavior. The second, but not the first, is a consequence of the discrete nature of the ladder. Within the flux-flow regime, there are also a series of steps, which are caused by locking of the solitons to phasonlike modes of the individual junctions; they are related to the finite length of the array, and secondarily to the fact that the ladder is a discrete rather than a continuum system. Finally, there is a “depinning” current for the solitons, which is nonzero only because one has a discrete, rather than a continuum sine-Gordon-like system.

Figure 1 shows our calculated IV characteristics with $\beta = 33$, $\eta_J = 1/\sqrt{2} = 0.71$, and several values of f . $\langle V \rangle$ denotes the space- and time-averaged voltage differences across the y junctions. There are two regimes, as mentioned above, both of which are also seen in simulations of the discrete sine-Gordon chain. The first is the

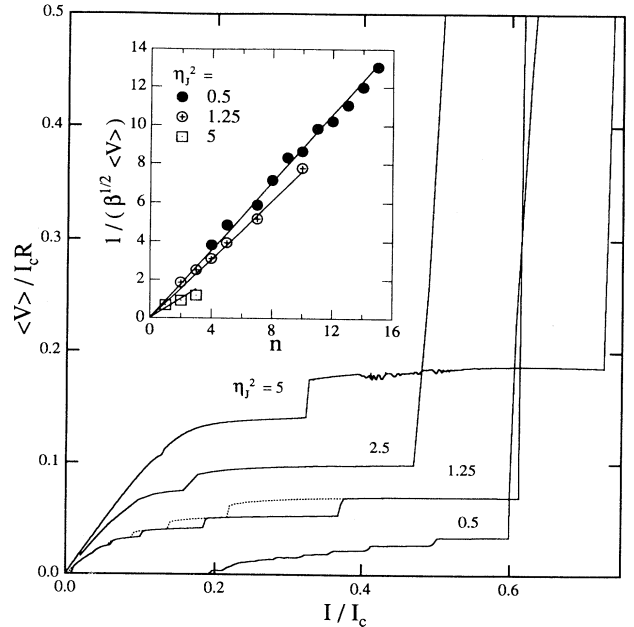


FIG. 2. Calculated IV curves for $f = 1/8$, $\beta = 61$, and several values of the anisotropy parameter η_J . The inset shows the voltages of steps corresponding to locking number n determined from our numerical result compared to those calculated from Eq. (4) (solid lines).

flux-flow regime where $\langle V \rangle(I, f)$ is roughly proportional to f (up to about $f=3/8$) and to I . In this regime, for each f , $\langle V \rangle(I, f)$ exhibits a series of voltage steps. The second regime corresponds to “resistance steps” in which $\langle V \rangle = RI$ independent of f , and is dominated by the whirling modes.

Figure 2 shows an expanded low-current regime for $f = 1/8$, $\beta = 61$, and several η_J 's. The voltage steps are very prominent. The IV characteristics are hysteretic on each of the steps, as shown with broken lines for $\eta_J^2 = 1.25$. Similar hysteretic steps are well known in numerical studies of the discrete sine-Gordon equation [1,2]. The critical current for the onset of voltage varies from about $0.2I_c$ at $\eta_J = 0.71$ to ≈ 0 for $\eta_J > 1$, in the less discrete regime, similar to results obtained in [3].

B. Soliton behavior

In the absence of damping and driving, the continuum version of Eq. (2) has, among other solutions, the sine-Gordon soliton [7], given by

$$\varphi_s(x, t) \sim 4 \tan^{-1} \left[\exp \left\{ (x - v_v t) / \sqrt{\eta_J^2 - \beta v_v^2} \right\} \right], \quad (7)$$

where v_v is the velocity. The phase in this soliton rises

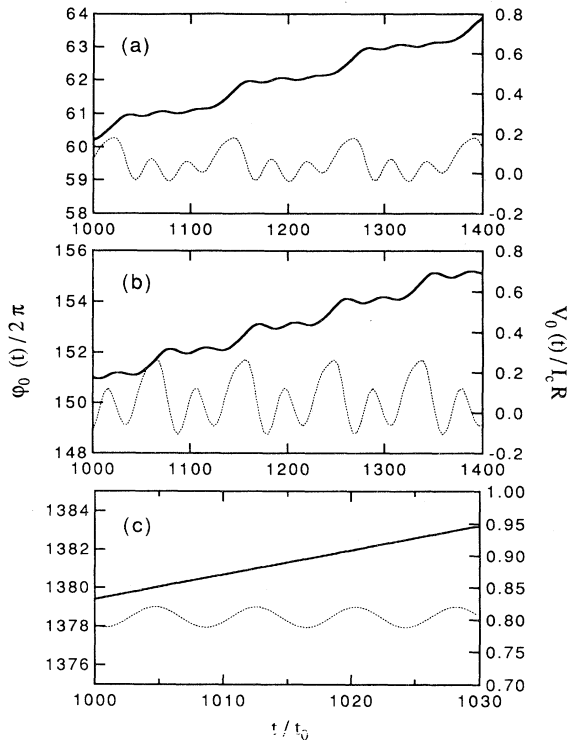


FIG. 3. Local phase difference $\varphi_i(t)$ (solid lines) and voltage $V_i(t)$ (broken lines) for $i = 0$, $f = 1/8$, $\eta_J^2 = 1.25$, $\beta = 61$, and three values of the applied current: $I/I_c = 0.22$ and 0.41 , corresponding to currents on voltage plateaus with $n = 3, 2$; and $I/I_c = 0.8$, corresponding to a current in the whirling regime. Note the different scales in the axes for the whirling regime.

from ~ 0 to $\sim 2\pi$ in a width $d_k \sim \sqrt{\eta_J^2 - \beta v_v^2}$. We will now show that, in the flux-flow regime, $\varphi(x, t)$ behaves much like such a soliton, but with characteristic modifications arising from coupling to local “phason” excitations, and from the discreteness of the lattice.

Figures 3(a) and 3(b) show the local phase difference $\varphi(x, t)$ for the Josephson ladder at two currents in the flux-flow regime (“region I”): $I/I_c = 0.22$ and 0.41 . The other parameters are $f = 1/8$, $\beta = 61$, and $\eta_J^2 = 1.25$. Both curves show clear solitonlike behavior, namely, an increase of $\varphi(x, t)$ in steps of $\approx 2\pi$ over a time interval d_k/v_v , as suggested by the sine-Gordon equation. The passage of the kink is accompanied by ripples arising from phason excitations. Typically, an integer number of ripple periods is found between successive kink passages. The local voltage $\dot{\varphi}(0, t)$ (shown as broken lines) in the flux-flow regime is due to such sine-Gordon solitons, modified by coupling to phasons. The larger peaks in the local voltage correspond to passage of the soliton or vortex (we have confirmed this by snapshots of the soliton motion in our simulations), while the decaying smaller peaks correspond to the phasons that couple to the vortex.

The step positions in Fig. 2 are determined by a locking of the vortex motion to these phasons. The phason dispersion relation is determined by linearizing the left-hand side of Eq. (2) with $i = 0$. The result is $\varphi_m(x, t) \propto \exp(-t/2\beta)e^{i(k_m x - \omega_m t)}$, where $\omega_m = \pm \sqrt{1 + 4\eta_J^2 \sin^2(k_m/2)}/\sqrt{\beta}$, as obtained previously by several groups [1,2]. The allowed wave vectors k_m are determined by periodic boundary conditions: $k_m = 2\pi m/N$, $m = 0, 1, 2, 3, 4, \dots$. To obtain the locking condition, note that the vortex circulates the ladder with frequency $\omega_v = 2\pi v_v/(Na)$. A resonance will occur if there are an integer number of phason cycles per vortex cycle. This condition gives $\omega_m = n\omega_v$ with $n = 1, 2, 3, \dots$, or

$$\frac{1}{\sqrt{\beta} \langle V \rangle} = \frac{n}{\sqrt{1 + 4\eta_J^2 \sin^2(\pi m/N)}}. \quad (8)$$

All the voltage steps we have found in Fig. 2 satisfy this condition. At $\eta_J = 0.71$, for example, we were able to identify resonances in the range $3 < n < 15$, $m = 1$, from a high-resolution IV characteristic and its derivatives. Presumably, the resonances corresponding to higher n are weaker because the phasons are damped, relaxing over a time 2β . At larger η_J , we can identify only a few values of n . The values of n for each step can also be found by enumerating the number of phason wavelengths between successive vortex passages, as in Figs. 3(a) and 3(b). In the inset of Fig. 2 we compare the positions of the steps thus located to the predictions of Eq. (7). In all cases, only the $m = 1$ mode is necessary to account for the resonances.

Figure 3(c) shows $\varphi(x, t)$ for the same ladder at a current in the “whirling” regime, $I/I_c = 0.8$ (“region II”). The other parameters are as in Figs. 3(a) and 3(b). In this regime, $\langle V \rangle \propto I$, and the local voltage oscillates sinusoidally in time. Each oscillation period again cor-

responds to the passage of a “vortex” through a given junction, as can be confirmed by the fact that the v_v thus found is consistent with the independently computed $\langle V \rangle$, via the Josephson relation.

The transition into the whirling regime occurs at $n_{\min} = 4, 2, 2, 1$ for $\eta_J^2 = 0.5, 1.25, 2.5, 5$. This can also be understood from the kink-phason resonance picture. To a phason mode, the passage of a kink of width d_k will appear like the switching on of a steplike driving current over a time of order d_k/v_v . The kink will couple to the phasons only if $d_k/v_v \geq \pi/\omega_1$, the half-period of the phason, or equivalently

$$\frac{1}{\sqrt{\beta}v_v} \geq \frac{\sqrt{1+\pi^2}}{\eta_J} = \frac{3.3}{\eta_J}. \quad (9)$$

This condition agrees very well with our numerical observations, even though it was obtained by considering soliton solutions from the continuum sine-Gordon equation, rather than the discrete sine-Gordon equation that we expect to apply here.

The fact that the voltage in the flux-flow regime is approximately linear in f can be qualitatively understood from the following argument. Suppose that φ for Nf fluxons can be approximated as a sum of well-separated solitons, each moving with the same velocity and described by $\varphi(x, t) = \sum_{j=1}^{Nf} \varphi_j$, where $\varphi_j = \varphi_s(x - x_j, t)$. Since the solitons are well separated, we can use following properties: $\sin[\sum_j \varphi_j] = \sum_j \sin \varphi_j$ and $\int \varphi_j \dot{\varphi}_i dx \propto \delta_{ij}$. By demanding that the energy dissipated by the damping of the moving soliton be balanced by the driving current providing $[\propto \int dx i \dot{\varphi}(x)]$ one can show that the Nf fluxons should move with the same velocity v as that for a single fluxon driven by the same current. This will lead to a voltage that is linear in f .

In the “whirling” regime, the f independence of the voltage can be understood from a somewhat different argument. Here, we assume a periodic solution of the form $\varphi = \sum_{j=1}^{Nf} \varphi_w(x - \tilde{v}t - j/f)$ moving with an unknown velocity \tilde{v} where $\varphi_w(\xi)$ describes a whirling solution containing one fluxon. Then using the property $\varphi(x + m/f) = \varphi(x) + 2\pi m$, one can show after some algebra that $\sin[\sum_{j=1}^{Nf} \varphi_w(x - \tilde{v}t - j/f)] = \sin[Nf \varphi_w(x - \tilde{v}t)]$. This means that $Nf \varphi_w(x - \tilde{v}t)$ is a solution to Eq. (2) as is $\varphi_w(x - vt)$. Finally, using the approximate property $\varphi_w(\xi) \sim \xi$ of the whirling state, one finds $\tilde{v} = v/(Nf)$, leading to an f -independent voltage.

C. Ballistic soliton motion and soliton mass

A common feature of massive particles is that they can move “ballistically.” That is, they continue to move under the influence of inertia even after the driving force has been turned off. Such propagation has been reported experimentally in certain novel geometries, such as a pair of square arrays linked by a narrower array [8]. As yet, however, to our knowledge, no such propagation has been found in numerical simulations in either square or triangular lattices [9–11].

We have sought such ballistic motion in the flux-flow regime of our ladder arrays. In isotropic ladders ($\eta = 0.71$), we again found no ballistic propagation, presumably because of the large pinning energies produced by the periodic lattice at this anisotropy. (The critical current for soliton depinning at $\eta_J = 0.71$ is about $0.2I_{cy}$, about twice that calculated for a square lattice [12].) However, at $\eta_J > 1$, we do observe ballistic motion in the flux-flow region I. As an example, Fig. 4 shows $V(t)$ and dV/dt at junction 0, for $\eta_J^2 = 5$, $I/I_c = 0.41$ (on the $n = 1$ voltage step), after the driving current is switched off at $t = 0$. The washboard-like ridges of V on a decreasing background, and perhaps more clearly, the spikes in dV/dt , correspond to a vortex passing through this junction. The increasing distance between peaks indicates that the vortex is slowing down. The vortex circulates at least five times around the ring before stopping—a fact that is also verified by direct observation of the vortex motion in real time. Qualitatively similar behavior was also observed for slower vortices on the lower current steps so long as $\eta_J > 1$. This behavior can be understood by noting that increasing η_J increases the width of the kink d_k , and thereby effectively makes the ladder seem *less* discrete. The fluxon at large η_J therefore has a much lower depinning current (as can also be seen from the curves in Fig. 2). Because of this lower depinning current, it can propagate ballistically.

We can define the fluxon mass in our ladder by equating the charging energy $E_c = C/2 \sum_{ij} V_{ij}^2$ to the kinetic energy of a soliton of mass M_v : $E_{\text{kin}} = \frac{1}{2} M_v v_v^2$ [10]. Since E_c can be directly calculated in our simulation, while v_v can be inferred from the calculated $\langle V \rangle$, this gives an unambiguous way to determine M_v . For the isotropic case $\eta_J^2 = 0.5$, we find $E_c/C \sim 110(\langle V \rangle / I_c R)^2$, in the flux-flow regime (region I of Fig. 1). This gives $M_v^f \sim 3.4C\phi_0^2/a^2$, more than six times the usual estimate for the vortex mass in a two-dimensional (2D) square lattice [13]. Similarly, the vortex friction coefficient γ can be estimated by equating the rate of energy dissipation, $E_{\text{dis}} = \frac{1}{2} \sum_{ij} V_{ij}^2 / R_{ij}$, to $\frac{1}{2} \gamma v_v^2$. This esti-

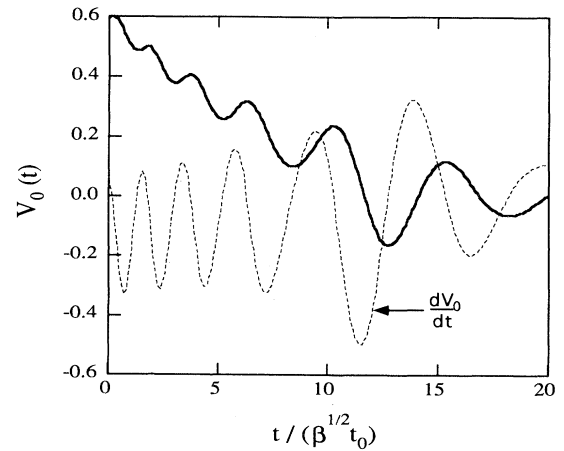


FIG. 4. Plot of $V_0(t)$ and $dV_0(t)/dt$ at $x = 0$ after driving current is turned off at time $t = 0$. We use $\eta_J^2 = 5$, and $I/I_c = 0.41$, corresponding to an $n = 1$ voltage plateau.

mate yields $\gamma^I \sim 3.4\phi_0^2/(Ra^2)$, once again more than six times the value predicted for 2D arrays [10]. This large dissipation explains the absence of ballistic motion for this anisotropy [10,11]. At larger values $\eta_J^2 = 5$ and 2.5, a similar calculation gives $M_v^I \sim 0.28$, and $0.34\phi_0^2/(Ra^2)$, $\gamma^I \sim 0.28$ and $0.34\phi_0^2/(Ra^2)$. These lower values of γ^I , but especially the low pinning energies, may explain why ballistic motion is possible at these larger values of η_J .

IV. DISCUSSION

We have presented numerical evidence showing that a Josephson ladder has dynamical properties very similar to those previously noted in a discrete sine-Gordon chain. Among the features we find in common are two distinct regions in the IV characteristics—a flux-flow regime and a “whirling” regime—and a series of steps arising from the locking of the sine-Gordon fluxons to “phason” or spin-wave-like modes of the individual junctions, which are quantized by the finite length of the ladder. We have also given an analytical argument that strongly suggests that the Josephson ladder should have discrete-sine-Gordon-like characteristics, provided certain inequalities are satisfied. The condition is basically that the sine-Gordon soliton should have a width substantially larger than the distance between junctions, so that the phase difference should vary slowly with coordinates along the ladder. Our argument is a dynamical generalization of one previously given by Kardar [5] for the energetics of a Josephson ladder.

Although the analytical argument that reduces the dynamics of the Josephson ladder to that of a discrete sine-Gordon chain involves a small-angle expansion of a phase difference [cf. Eq. (2)] the resulting equation still retains effects of discreteness, which can clearly be seen in our numerical results. The most obvious of these are (i) the existence of a finite depinning current for the fluxons (this depinning current would vanish in the continuum limit) and (ii) the existence of the “whirling” regime (which would not occur in the continuum sine-Gordon equation, as already noted in [2]).

Because of the analogy between Josephson ladders and discrete sine-Gordon systems, one can draw interesting connections between corresponding parameters in the two models. For example, the anisotropy parameter η is equivalent to the inverse of a discretization parameter

used in discrete sine-Gordon systems. This suggests that a Josephson ladder with high anisotropy should behave more nearly like a continuum sine-Gordon system than one with low anisotropy. Indeed, we can see that this is true, especially as regards the magnitude of the vortex depinning current I_d . Although we have no good analytical theory for I_d at present, our numerical results show that it is nearly zero for anisotropies $\eta > 1$, while it is very substantial ($> 0.2I_{cy}$) for isotropic ladders ($\eta = 0.71$). In this case, the appropriate continuum sine-Gordon system for comparison is a long Josephson junction, which indeed is intuitively the natural limit of an anisotropic ladder.

Although the anisotropy parameter η might appear to be an unnecessary complication to the already complex physics of a Josephson ladder, it is clearly a useful means for tuning the transition from discrete to continuum behavior in a ladder. Thus it might be viewed by experimentalists as worth varying in the laboratory [14]. For example, one interesting experimental possibility would be to control the vortex depinning current and effective mass by manipulation of the anisotropy in the Josephson coupling.

Finally, we comment briefly on the possible relevance of these results to *two-dimensional* Josephson networks. Clearly, Josephson ladders and discrete sine-Gordon chains are unique, as well as extraordinarily rich and complicated systems; most of their properties cannot be extrapolated to two-dimensional systems. Nonetheless, it is intriguing that several features of Josephson ladder dynamics also show up in simulations of underdamped two-dimensional arrays [9–11,15]. These are the flux-flow regime, initiated by a finite critical current; the locking of vortices (the analogs of solitons) to phasons, and the existence of resistance steps (the analogs of whirling modes). It remains to be seen whether this connection has more than accidental significance.

ACKNOWLEDGMENTS

We are grateful for valuable conversations with A. V. Ustinov. This work has been supported by NSF Grant No. DMR94-02131 and by the Midwest Superconductivity Consortium through DOE Grant No. DE-FG02-90ER-45427. S.R. received financial support from Ohio State University.

-
- [1] A. V. Ustinov, M. Cirillo, and B. A. Malomed, *Phys. Rev. B* **47**, 8357 (1993); A. V. Ustinov *et al.*, *ibid.* **51**, 3081 (1995).
 - [2] S. Watanabe, S. H. Strogatz, H. S. J. van der Zant, and T. P. Orlando, *Phys. Rev. Lett.* **74**, 379 (1995).
 - [3] H. S. J. van der Zant, Terry P. Orlando, Shinya Watanabe, and Steven H. Strogatz, *Phys. Rev. Lett.* **74**, 174 (1995).
 - [4] K. Nakajima *et al.*, *J. Appl. Phys.* **66**, 949 (1989); K. Likharev and V. Semenov, *IEEE Trans. Appl. Suppl.* **AS-1**, 3 (1991); J. H. Miller *et al.*, *Appl. Phys. Lett.* **59**, 3330 (1991).
 - [5] Mehran Kardar, *Phys. Rev. B* **33**, 3125 (1986).
 - [6] See, for example, S. R. Shenoy, *J. Phys. C* **18**, 5163 (1985); A. Falo *et al.*, *Phys. Rev. B* **41**, 10983 (1991); R. Bhagavatula *et al.*, *ibid.* **45**, 4772 (1992); W. Yu *et al.*, *ibid.* **45**, 12624 (1992).
 - [7] R. Rajaraman, *Solitons and Instantons* (North-Holland, Amsterdam, 1982).
 - [8] H. S. J. van der Zant *et al.*, *Europhys. Lett.* **18**, 343 (1992).
 - [9] P. A. Bobbert, *Phys. Rev. B* **45**, 7540 (1992).

- [10] U. Geigenmüller, C. J. Lobb, and C. B. Whan, Phys. Rev. B **47**, 348 (1993).
- [11] Wenbin Yu and D. Stroud, Phys. Rev. B **49**, 6174 (1994).
- [12] C. J. Lobb, D. W. Abraham, and M. Tinkham, Phys. Rev. B **27**, 150 (1983).
- [13] H. S. J. van der Zant *et al.*, Phys. Rev. B **47**, 295 (1993).
- [14] Indeed, many laboratory-prepared Josephson ladders, nominally isotropic, will undoubtedly have *random* anisotropy as a result of random variations in both I_{cx} and I_{cy} , which would probably produce a variety of unusual behaviors.
- [15] H. R. Shea, M. A. Itzler, and M. Tinkham, Phys. Rev. B **51**, 12690 (1995) have shown numerically that overdamped, hybrid 2D arrays can be modeled as an anisotropic network of coupled RSJ's.